

Kinematics of the Broad Line Region in M81

Nick Devereux¹

Department of Physics, Embry-Riddle Aeronautical University, Prescott, AZ 86301

devereux@erau.edu

and

Andrew Shearer

Physics Department, National University of Ireland, Galway

andy.shearer@nuigalway.ie

ABSTRACT

A new model is presented which explains the origin of the broad emission lines observed in the LINER/Seyfert nucleus of M81 in terms of a steady state spherically symmetric inflow, amounting to $\sim 1 \times 10^{-5} M_{\odot}/\text{yr}$, which is sufficient to explain the luminosity of the AGN. The emitting volume has an outer radius of ~ 1 pc, making it the largest broad line region yet to be measured, and it contains a total mass of $\sim 5 \times 10^{-2} M_{\odot}$ of dense, $\sim 10^8 \text{ cm}^{-3}$, ionized gas, leading to a very low filling factor of $\sim 5 \times 10^{-9}$. The fact that the BLR in M81 is so large may explain why the AGN is unable to sustain the ionization seen there. Thus, the AGN in M81 is not simply a scaled down quasar.

Subject headings: galaxies: Seyfert, galaxies: individual(M81, NGC 3031), quasars: emission lines

1. Introduction

Broad emission lines (Seyfert 1943) are a defining characteristic of active galactic nuclei (AGN). They occur in AGNs spanning seven decades in luminosity, from the lowest luminosity Seyferts to the highest luminosity quasars. A variety of models have been proposed

¹Fulbright Scholar, Physics Department, National University of Ireland, Galway

to explain the origin of the broad emission lines, but they all have one feature in common; that the lines are formed in the dense, $\sim 10^8$ to 10^9 cm^{-3} , and fast moving, $\sim 10^4$ km/s, gas, close to a massive black hole (MBH) (Rees 1977). The models differ only in how the gas achieves it's high velocity, be it through inflow, outflow, spinning in a disk or attached to stars orbiting close to the AGN. Identifying the mechanisms that produce broad emission lines is of paramount importance as only then will we finally be able to understand, and exploit, the physics of the small and as yet, spatially unresolved broad emission line regions (BELRs) in galaxies.

The main purpose of this paper is to draw attention to an important subset of AGNs that exhibit flat-topped broad emission line profiles which may be utilized to determine a size for the broad line region (BLR) that heretofore has previously only been possible using reverberation mapping techniques (Peterson (1993), Peterson (2001)). We demonstrate the utility of this new technique by interpreting the flat-topped broad $\text{H}\alpha$ emission line profile of the LINER/Seyfert nucleus of M81.

At a distance of 3.6 Mpc (Freedman et al. 2001) M81 contains the nearest and best resolved low luminosity AGN (Peimbert & Torres-Peimbert (1981), Filippenko & Sargent (1988)). The almost face-on aspect of the host galaxy allows a clear and unobscured view of the nucleus which has been studied across the electromagnetic spectrum (Peimbert & Torres-Peimbert (1981), Ho, Filippenko & Sargent (1996), Bower et al. (1996), Bietenholz, Bartel & Rupin (2000), La Parola et al. (2004)). M81 harbors a black hole (BH) with a mass, $M_{BH} = 7 \times 10^7 M_{\odot}$, deduced from a two dimensional velocity map obtained with STIS on the HST (Devereux et al. 2003). The AGN is identified with a UV point source at the nucleus which has a luminosity at 1500 Å, $L_{1500} = 5 \times 10^5 L_{\odot}$ (Devereux, Ford & Jacoby 1997) and an X-ray (0.5 - 2.4 keV) luminosity of $5 \times 10^6 L_{\odot}$ (La Parola et al. 2004).

Our paper is based on the premise that the broad emission lines (BELs) are produced in a kinematically distinct and hence physically distinct region centered on the BH. Therefore, the broad emission line region (BELR) has a well defined inner radius and outer radius. Since the gravitational field strength is already known in M81, the relationship between velocity and radius may be established, given a kinematic model for the BELR gas. Thus, in principle, one can determine the inner and outer radii of the BELR in M81 by modeling the broad emission line profiles.

The layout of our paper is as follows. In section 3, we evaluate the origin of the BELs seen in M81 in the context of viable models for the production of BELRs in AGNs, namely inflow, outflow, rotating gas disks and the atmospheres of stars illuminated by the AGN. In section 4, we discuss the viable models in the context of various constraints and conclude, in section 5, that inflow provides the best explanation for the BELR in M81. We begin,

however, with a review of the broad $H\alpha$ emission line observed in M81.

2. The Broad $H\alpha$ Emission Line Profile in M81

The broad $H\alpha$ emission line, measured by STIS aboard the HST, has been presented previously (Devereux et al. 2003) and is shown in Figure 1 for convenience. As the figure illustrates, the profile exhibits a rather unusual ‘flat-top’, that is rarely seen in AGNs. Such profiles may be produced by radiation from a spherically symmetric shell of gas in radial motion as noted previously by Capriotti, Foltz & Byard (1980). Single peaked emission line profiles may also be produced by accretion disks (Chen & Halpern 1989) and bipolar flows (Zheng, Binette & Sulentic 1990).

As reported in Devereux et al. (2003), the entire broad $H\alpha$ line is redshifted by $\sim 7 \text{ \AA}$ ($\sim 300 \text{ km/s}$) with respect to the narrow $H\alpha$ line. The broad line is very symmetrical and so the redshift can not be attributed to skewness in the line shape. Similar redshifts have been noted for broad emission lines in other AGNs (Eracleous & Halpern 2003). We presently have no explanation for this phenomenon, and we overlook it for now, with the consequence that the velocities reported in this paper are relative to the center of the respective emission lines.

Slight irregularities on the redward side of the profile, near the peak, coincide with the narrow components of the 6563 \AA $H\alpha$ line and the brighter of the two [NII] lines, each of which had to be subtracted to isolate the broad $H\alpha$ component, as described in more detail by Devereux et al. (2003). The blue side of the profile, however, is less susceptible to the subtraction procedure because it coincides with the fainter [NII] line. Interestingly, the $H\beta$ line is similar in shape to the $H\alpha$ emission line as noted previously by Filippenko & Sargent (1988) and Bower et al. (1996). The distinctive ‘flat-top’ is thus well established for M81. Other broad emission lines are observed in M81, as described previously by Ho, Filippenko & Sargent (1996), but the Balmer lines are the brightest, they are presently the best resolved spectrally and hence the easiest to model.

The broad Balmer lines in M81 are apparently variable. Faint, widely separated ‘double peaks’ did appear on the wings of the Balmer lines as reported previously by Bower et al. (1996), but they did not appear in the more recent STIS spectrum. The transient features are consistent with the disruption of a star at the tidal radius of the MBH in M81, but the broad line itself remains to be explained.

3. Broad Line Region Models

A large body of work exists addressing the origin of broad lines in luminous AGNs, but the problem of the formation and confinement (Mathews & Ferland 1987), the excitation (Kwan & Krolik 1981) and the kinematics (Robinson, Perez, & Binette 1990) of the broad line gas remains unsolved. Interestingly, broad lines also occur in low luminosity AGNs (Filippenko & Sargent 1985) which presents the opportunity to examine the phenomenon from a different perspective. Furthermore, rather than attempting to explain the observed properties of *all* low luminosity AGNs, we approach the problem from the point of view of examining one well studied example, namely M81.

3.1. Outflow Model

Evidence for outflow is seen in the spectra of broad absorption line quasars (e.g. Hazard et al. (1984), Arav et al. (1999)). However, the outflow model can be ruled out for M81 because the diminutive luminosity generated by the AGN is simply unable to provide sufficient radiation pressure to overcome the gravitational force of the MBH as demonstrated in the following.

The condition for a radiatively driven wind is given by,

$$\kappa L/4\pi cG > M \tag{1}$$

where M and L are the mass and luminosity respectively, interior to a radius r , c is the speed of light, and G the gravitational constant. For M81, this condition is not satisfied by six orders of magnitude, if one adopts the Thompson scattering opacity $\kappa = 0.4 \text{ cm}^2/\text{g}$ for a pure hydrogen gas, $M_{BH} = 7 \times 10^7 M_{\odot}$, and a combined UV and X-ray luminosity of $5 \times 10^6 L_{\odot}$. The disparity is simply too large to overcome even by invoking line opacities, as line driven winds are viable only for objects that radiate close to the Eddington luminosity limit (King & Pounds (2003), Shlosman, Vitello, & Shaviv (1985)). A short, $1.7 \times 10^{-2} \text{ pc}$, one sided radio jet (Bietenholz, Bartel & Rupin 2000) is seen to emerge from the nucleus of M81, but this is an unlikely source for the observed broad line emission as that outflow consists of a relativistic plasma.

3.2. Stellar Atmospheres Illuminated by the Central AGN Model

We are also able to rule out another contending theory for the production of broad emission lines in M81, namely ionization of the extended mass loss envelopes of red giant stars orbiting close to the AGN (eg. Scoville & Norman (1988), Alexander & Netzer (1997)). Stellar winds provide a natural explanation for the confinement and replenishment of the so called ‘broad line clouds’, which is otherwise a major problem (Mathews & Ferland 1987). However, such a model is unlikely to be the explanation for the BELR in M81, because the intensity of ionizing photons at the tidal radius is insufficient to penetrate the denser, $\sim 10^8 \text{ cm}^{-3}$, region of the mass loss wind, as shown in the following.

The tidal radius, R_{tidal} , for stars in synchronous rotation around a BH is given by

$$R_{tidal} = R_{star} [M_{BH}/M_{star}]^{1/3} \quad (2)$$

For a $1 M_{\odot}$ star of radius 10^{13} cm , in the vicinity of a $7 \times 10^7 M_{\odot}$ BH, the tidal radius corresponds to $4 \times 10^{15} \text{ cm}$.

Following Scoville & Norman (1988), and assuming plane parallel geometry, the ionizing photon flux at the tidal radius is related to the penetration depth, d , in the inverted Stromgren sphere of the stellar wind by

$$\int_d^{\infty} \alpha_B n_H^2 dr = \int_{\nu_o}^{\nu_{max}} [L/(4\pi R_{tidal}^2 h\nu)] d\nu \quad (3)$$

where $\alpha_B = 2.6 \times 10^{-13} \text{ cm}^{-3} \text{ s}^{-1}$, is the Case B recombination coefficient, and $h\nu$ is the energy of an ionizing photon.

For a power law of spectral index α ,

$$L = L_o (\nu/\nu_o)^{-\alpha} \quad (4)$$

the right hand side of equation 3 integrates to

$$\int_d^{\infty} \alpha_B n_H^2 dr = L_o \nu_o^{\alpha} [\nu_o^{-\alpha} - \nu_{max}^{-\alpha}] / (h\alpha 4\pi R_{tidal}^2) \quad (5)$$

The hydrogen number density, n_H , is related to the stellar mass loss rate, \dot{M} , and the wind velocity, v_W , via the equation of continuity;

$$n_H(r) = \dot{M}/(4\pi r^2 v_W m_H) \quad (6)$$

Combining equations 3 and 6, and evaluating the left hand integral, one finds,

$$d = [R_{tidal}^2 \alpha_B h \alpha \dot{M}^2 / (4\pi L_o \nu_o^\alpha [\nu_o^{-\alpha} - \nu_{max}^{-\alpha}] v_W^2 m_H^2)]^{1/3} \quad (7)$$

Substituting equation 7 into equation 6, and adopting $\alpha = 2$, $h\nu_o = 13.6$ eV and $h\nu_{max} = 600$ eV (Ho, Filippenko & Sargent 1996), one obtains for the number density in the wind, n , at the penetration depth, d , of the ionizing photons;

$$n(d) = 63 \times 10^6 [L_{1500}/10^5 L_\odot]^{2/3} [R_{tidal}/10^{15} cm]^{-4/3} [v_W/10 km/s]^{1/3} [\dot{M}/10^{-5} M_\odot/yr]^{-1/3} cm^{-3} \quad (8)$$

Substituting representative values for the wind velocity $v_W = 10$ km/s, and stellar mass loss rates of $\dot{M} = 10^{-5} M_\odot/yr$ (Scoville & Norman 1988) and $\dot{M} = 10^{-6} M_\odot/yr$ (Alexander & Netzer 1997), one finds for M81 that representative densities in the wind at the penetration depth of the ionizing photons are $30 \times 10^6 cm^{-3}$ and $63 \times 10^6 cm^{-3}$, respectively. Thus, the density where most of the H α emission is produced is expected to be significantly lower than the $\sim 10^8 cm^{-3}$ required for the broad line region of M81 to not produce broad forbidden lines (Ho, Filippenko & Sargent 1996). Furthermore, the densities calculated above are for stars as close to the UV source as the tidal radius permits, and assume no absorption of ionizing photons inside that volume. Obviously, the penetration depths and densities will be lower for the majority of stars which are further away. Plus, it is quite likely that there is gas inside the tidal radius that would attenuate the ionizing flux, thereby exacerbating the problem. An additional argument against stars is that, for M81, the emitting envelopes would occupy such a narrow range of orbital velocities that they would be unable to reproduce the observed broad line profile. We therefore conclude that the BELR in M81 is not produced by the extended mass loss envelopes of red giant stars orbiting close to the AGN.

3.3. Accretion Disk Model

The next contender for the origin of the broad emission lines is a rotating 'accretion disk'. While there has been a novel proposal (Murry & Chiang 1997) to generate a single peaked profile using a disk wind, we are reluctant to adopt it as there is no *a priori*

evidence that there is an outflowing wind in M81. Instead, the model used here involves a relativistic accretion disk developed by Chen & Halpern (1989), and adopted later by Eracleous & Halpern (2001) to explain the single peaked broad line profile in the LINER nucleus NGC 3065. An illustrative fit to the broad H α emission line in M81, using the relativistic disk model, is presented in Figure 2.

The model invokes five free parameters, a dimensionless inner radius, ζ_1 , and outer radius, ζ_2 , an inclination angle, i , an emissivity law, q , and a velocity dispersion for the gas, σ . As described previously by Eracleous & Halpern (2001), the two emission peaks; a distinguishing characteristic of disk models, may be merged into a single peak, and the profile wings made symmetric, if the disk has a large outer radius and is inclined to the line of sight. The model also incorporates a 300 km/s velocity dispersion to widen the two velocity peaks so that they merge into a reasonable representation of the flat-top profile seen in M81. Additionally, the model incorporates a $q=2$ emissivity law which accentuates emission from the inner regions of the disk. For a BH with a mass the same as measured for M81, the outer radius of the disk model, illustrated in Figure 2, is large, corresponding to ~ 0.8 pc.

The success of the model in fitting the profile is dependent on the disk inclination. If the disk is nearly face-on, as observed for the narrow line gas (Devereux et al. 2003), then the inner radius of the disk has to be small to achieve the necessary range of velocities at zero intensity. Consequently, gravitational and transverse redshifts become discernable, with the result that the red wing becomes asymmetric, somewhat extended and unlike the observed profile. However, a disk inclination of 50 degrees is able to reproduce the shape of the M81 profile quite well as Figure 2 illustrates. Such a high inclination for the inner disk is supported by observations of the radio jet (Bietenholz, Bartel & Rupin 2000). Thus, if the broad emission line is produced by an accretion disk, then the unresolved inner part of the disk is considerably more inclined than the larger scale disk seen in ground based and space based images.

3.4. Evidence for Inflowing Gas In M81

As alluded to in the introduction, a steady state spherical inflow is also able to reproduce the broad H α emission line profile observed for M81, and with the minimum of assumptions. The relationship between velocity and radius is determined by the mass distribution, $M(r)$, to be

$$v(r) = -\sqrt{2GM(r)/r} \tag{9}$$

where $M(r)$ includes a point mass, representing the black hole, embedded in the center of an extended star cluster, as described previously by Devereux et al. (2003). The observed, radial component, of the velocity for each particle, i , is given by

$$v_i = v(r)\cos\Theta \quad (10)$$

where Θ is the angle between the radial velocity vector and the line of sight.

A broad line profile, $\Phi(v)$, with the characteristics of the one observed in M81 may be produced by generating a histogram of velocities for a system of particles distributed randomly within a spherical volume bounded by an inner radius, r_{inner} , an outer radius, r_{outer} and a cloud number density distribution, $N(r)$, such that,

$$\Phi(v) = \sum_{r_{inner}}^{r_{outer}} N(r)v_i \quad (11)$$

For a steady state flow, where $\dot{M} \neq f(r)$, the cloud number density distribution is determined by mass conservation to be,

$$N(r) \propto r^{-3/2} \quad (12)$$

As described previously by Capriotti, Foltz & Byard (1980), the velocity width of the ‘flat-top’ is determined by the outer radius, and the width at zero intensity is determined by the inner radius. Thus, given a density distribution and a velocity law, one can use the profile shape to determine the physical size of the emitting region. Values that reproduce the best representation of the broad H α emission line profile, shown in Figure 1, correspond to an outer radius, $r_{outer} = 1$ pc, and an inner radius, $r_{inner} = 0.2$ pc.

There are other broad lines seen in M81, but they are fainter and were acquired with lower spectral resolution. However, two of the better examples appear in the UV; Ly α at 1216 Å and Mg II at 2800 Å. They are reproduced in Figures 3 and 4 respectively. According to Ho, Filippenko & Sargent (1996), the central depression seen in the Ly α line is likely caused by interstellar absorption and the bright central narrow line is geocoronal emission. They suggest that interstellar absorption is also responsible for the structure seen in the core of the Mg II line. Nevertheless, the *wings* of the Ly α and Mg II profiles can be reproduced using the same inflow model and yield slightly different sizes for the emitting region. For example, the Ly α emission line requires $r_{outer} = 0.7$ pc, and an inner radius, $r_{inner} = 0.1$ pc. The Mg II emission line requires $r_{outer} = 0.9$ pc, and an inner radius, $r_{inner} = 0.35$ pc. These

illustrative fits are shown in Figures 3 and 4. Overall, the sizes determined for the BELRs are similar. We note that the line width at the intensity of the continuum sets an upper limit on the inner radius. This is because the line may well persist below the continuum level, even though it can not be directly measured.

4. Discussion

Evidently, two plausible models; a rotating accretion disk and a spherically symmetric inflow, are able to reproduce the shape of the broad H α emission line profile observed for M81. In either case, the velocity law dictates that the emitting region is large; ~ 0.7 to 1 pc in radius. In the context of the accretion disk model, the broad H α emission line presumably represents the continuation of the larger scale H α disk, seen in ground based and space based images (Devereux, Ford & Jacoby 1997), as it extends down into the unresolved nuclear region. On the other hand, the interpretation of the broad H α emission line profile in terms of a spherically symmetric inflow would represent a new phenomenon for M81.

4.1. Broad Line Region Size

Perhaps the most surprising result to have emerged from our analysis is the large outer radius, ~ 1 pc, inferred for BELR of M81, regardless of whether the broad emission line is produced by an accretion disk or an inflow. With an angular diameter of $0.1''$, the BLR of M81 is on the brink of being resolved with HST. The large outer diameter inferred for the BLR may explain why a 'flat-top' profile is observed in M81, and rarely in other AGNs. Unless the BELR is resolved, the line profiles will be contaminated by the slower moving gas surrounding the BELR, causing the line profiles to be peaked rather than flat.

The size we infer for the BELR causes M81 to not conform to the correlation between BLR size and UV luminosity established for higher luminosity AGNs (Peterson (2001), Peterson (1993)). However, as noted by Kaspi, et al. (2005), the correlation appears to break down for low luminosity AGNs, with $L_{UV} \lesssim 10^6 L_{\odot}$, which would include M81. But the large size that we infer for the BELR of M81 does make it the largest ever measured. On the other hand, there are good reasons to believe the sizes of broad line regions may have been underestimated, previously, using the reverberation mapping technique, which is most sensitive to measuring the inner radius, closest to the AGN (Edelson & Krolik (1988), Robinson & Perez (1990)).

4.2. Broad Line Region Ionization

The size we infer for the BELR in M81 is orders of magnitude larger than the range of values cited by Ho, Filippenko & Sargent (1996) but their estimate is based on the *excitation parameter* which links the excitation of the broad emission lines to the central UV source. However, as noted previously by Ho, Filippenko & Sargent (1996) and Maoz et al. (1998) the nuclear UV source in M81 produces insufficient ionizing photons to explain the luminosity of the broad H α line, by a factor of 11 according to our calculations. We find that the the central AGN produces 9×10^{49} ionizing ph/s, integrated between 13.6 and 600 eV, assuming a ν^{-2} power law, whereas excitation of the broad H α emission line requires 1×10^{51} ionizing ph/s. Ho, Filippenko & Sargent (1996) also note that the BLR does not respond to time variable X-ray emission. In our view, this provides further evidence that the central AGN is not responsible for ionizing the BLR gas. That the BELR in M81 is so large may explain why the central AGN is unable to sustain the ionization seen there. Thus, the low luminosity AGN in M81 is not simply a scaled down quasar.

The origin of the excitation for the BELR is as enigmatic as the origin of the excitation for the more extended narrow line region in M81, discussed previously by Devereux, Ford & Jacoby (1997). Most likely, the gas is excited, in situ, by shocks, or by hot, and as yet undetected, PAGB stars. In either case, the excitation parameter would then be completely unrelated to the central source, and hence would not yield a useful measure of the BELR size.

4.3. Virial Black Hole Masses

Previous attempts to estimate the BH mass in M81 using the so called ‘Virial Method’ (Peimbert & Torres-Peimbert (1981), Filippenko & Sargent (1988), Ho, Filippenko & Sargent (1996)) have consistently underestimated the kinematically determined mass (Devereux et al. 2003) by factors ranging from 20 to 200. For example, the recent formalism of Greene & Ho (2005), which uses the FWHM *and* luminosity of the broad H α emission line, underestimates the mass of the BH in M81 by a factor of 140. On the other hand, the BH in M81 does conform to the BH mass-bulge velocity dispersion correlation (Ferrarese & Merritt 2000) as noted previously by Devereux et al. (2003). This dichotomy is regarded as further evidence that the BLR in M81 is very different from those studied in more luminous AGNs.

4.4. The Mass of Ionized Gas in the BELR of M81

The mass of emitting gas may be deduced from standard (Case B) recombination theory;

$$M_{emitting} = L(H_\alpha)m_H/n_H\alpha_{H\alpha}^{eff}h\nu_{H\alpha} \quad (13)$$

Using an effective recombination coefficient $\alpha_{H\alpha}^{eff} = 8.6 \times 10^{-14} \text{ cm}^{-3} \text{ s}^{-1}$, assuming a *constant* average density $n = 10^8 \text{ cm}^{-3}$, and a luminosity $L(H_\alpha) = 3.7 \times 10^5 L_\odot$ based on the broad line flux reported in Devereux et al. (2003), one finds $M_{emitting} = 0.05 M_\odot$. This mass is implausibly small for an accretion disk, but can be more easily reconciled with an inflow as shown in the following.

4.5. The Filling Factor and the Inflow Rate for the BELR of M81

It is straight forward to calculate the filling factor, ϵ , once the dimensions of the emitting region have been established. For a uniform density medium occupying a spherical volume of radius r , one finds

$$\epsilon = 3L(H_\alpha)/4\pi n_H^2 \alpha_{H\alpha}^{eff} h\nu_{H\alpha} r^3 \quad (14)$$

Again, using an effective recombination coefficient $\alpha_{H\alpha}^{eff} = 8.6 \times 10^{-14} \text{ cm}^{-3} \text{ s}^{-1}$, assuming a *constant* average gas density $n = 10^8 \text{ cm}^{-3}$, and a luminosity $L(H_\alpha) = 3.7 \times 10^5 L_\odot$ based on the broad line flux reported in Devereux et al. (2003), one finds $\epsilon \sim 5 \times 10^{-9}$ for M81.

Having established the dimensions of the emitting region and the filling factor one can now calculate the mass inflow rate for the ionized gas, using the equation of continuity;

$$\dot{M} = \epsilon 4\pi r^2 v(r) n_H(r) m_H \quad (15)$$

The velocity at the inner radius of 0.2 pc is determined by the mass distribution to be 1764 km/s. Setting the gas density in the flow to be 10^8 cm^{-3} one obtains a mass inflow rate, $\dot{M} = 1 \times 10^{-5} M_\odot/\text{yr}$. If the gas density is higher, the mass inflow rate will decrease. Conversely, if only a fraction of the inflowing gas is ionized, then the *total* mass inflow rate will, of course, be higher.

4.6. The Luminosity of the AGN

A variety of models have been considered for the production of the broad $H\alpha$ emission line in M81, but by far the most straight forward model, that involves the minimum of

assumptions, is the inflow model. Accretion onto a compact massive object has long been suspected as the origin for the luminosity of the AGN in M81 (Peimbert & Torres-Peimbert 1981) and recognizing the shape of the broad line profile may be the signature of an inflow permits us to corroborate this idea. According to the virial theorem, the maximum power, P , produced from the conversion of gravitational potential energy as material falls from a distance of 1pc, which for the purposes of this calculation is effectively at infinity, onto the event horizon of a MBH, can be expressed as

$$P = \dot{M}c^2/4 \tag{16}$$

A lower limit to the mass inflow rate that we infer from the ionized gas, $10^{-5} M_{\odot}/\text{yr}$, sets a lower limit of $4 \times 10^7 L_{\odot}$ for the power, P , which, without explaining the details, is sufficient to account for both the UV and X-ray luminosity of the AGN with a conversion efficiency of power into radiative luminosity of $\leq 14\%$. Interestingly, the mass inflow rate that we infer is also sufficient to sustain the radio jet according to Bietenholz, Bartel & Rupin (2000).

4.7. The Origin of the Broad Line Gas

If the broad emission lines are produced by an inflow, then one wonders how the incredibly small mass of gas in the BELR, measured to be $5 \times 10^{-2} M_{\odot}$, is distributed within the, by comparison, rather large emitting volume ~ 1 pc in radius. One can get an approximate estimate based on the 'noise' in the profile, as first suggested by Capriotti, Foltz & Byard (1981). The fact that the observed broad line profile is smoother than the model profile, which was generated using 75,000 points (see Figure 1) suggests that, on average, the mass of each 'broad line cloud' is $\lesssim 10^{-6} M_{\odot}$. We surmise that representative masses for broad line clouds $\sim 10^{-9} M_{\odot}$, cited previously by Alexander & Netzer (1994), are not at all unreasonable given that the observed profile in M81 is, in fact, so smooth.

It is not surprising, given the small mass of gas and the very low volume filling factor, that the *internal* extinction is negligible to both the UV source (Ho, Filippenko & Sargent 1996) and the gas responsible for the broad Balmer lines (Filippenko & Sargent (1988), Bower et al. (1996)). The fact that the $H\alpha$ profile is symmetric provides further evidence that the extinction to the BELR is inconsequential; apparently a common feature among AGNs (eg. Collin-Souffrin & Lasota (1988)).

We speculate that mass loss from a spherically symmetric distribution of late-type bulge stars may provide a more than adequate supply for the in-falling gas. Any gas for which the vector cross product

$$r \times p = 0 \tag{17}$$

where r is the radius vector and p is the linear momentum of the gas, will fall into the nucleus. Calculating how much gas satisfies this identity and furthermore, how it becomes so compressed, is beyond the scope of the present paper, but we note that only a small mass inflow rate, $\sim 10^{-5} M_{\odot}/\text{yr}$, of dense, 10^8 cm^{-3} , gas is required to explain the luminosity of the AGN.

5. Conclusions

We have demonstrated a new technique that has allowed us to determine the size of the broad line region (BLR) in M81 by modeling the shape of the broad line profile using a kinematic model for the broad emission line gas. Our principle conclusion is that the BLR is large, ~ 2 pc in diameter, regardless of whether the velocity field is represented by an accretion disk or a spherically symmetric inflow.

The fact that the BLR in M81 is so large may explain why the AGN is unable to sustain the ionization seen there. We therefore conclude that the gas responsible for the broad emission lines seen in M81 must be ionized in-situ, either by shocks, hot stars, or a combination of the two. Thus, the AGN in M81 is not simply a scaled down quasar.

How the gas becomes so compressed as to prevent the formation of broad forbidden lines remains a mystery. Nevertheless, if the gas density really is high, $\sim 10^8 \text{ cm}^{-3}$, then the broad $H\alpha$ emission line observed in the LINER/Seyfert nucleus of M81 is most easily understood in terms of a steady state spherically symmetric inflow, amounting to $\geq 1 \times 10^{-5} M_{\odot}/\text{yr}$, which is sufficient to sustain the luminosity of the AGN and the radio jet. We further speculate, based on the smoothness of the broad emission line profile, that the individual regions of dense ionized gas have masses $\lesssim 10^{-6} M_{\odot}$. Alternatively, if the gas density is significantly lower, then the total mass of gas increases, making the interpretation of the broad emission lines in terms of an accretion disk more amenable, but then explaining the absence of broad forbidden lines becomes a problem. Thus, the gas density remains pivotal in understanding the origin of the broad emission lines seen in M81.

The authors thank Dr. Luis Ho for providing digitized spectra, two of which were reproduced here. The authors also thank Prof. Mike Eracleous for his generous help with the relativistic accretion disk modeling. N.D. gratefully acknowledges the support of the Fulbright Commission and the hospitality of the National University of Ireland, Galway, where

this work was completed. The authors also gratefully acknowledge the support of the HEA funded Cosmogrid programme, and the referee for prompting us to consider the accretion disk model more carefully. This research has made extensive use of NASA's Astrophysics Data System.

Facilities: HST (STIS)

REFERENCES

- Alexander, T., & Netzer, H., 1994, MNRAS, 270, 781
- Alexander, T., & Netzer, H., 1997, MNRAS, 284, 967
- Arav, N; Becker, R. H., Laurent-Muehleisen, S. A., Gregg, M. D., White, R. L., Brotherton, M. S., de Kool, M., 1999, ApJ 524, 566
- Bietenholz, M.F., Bartel, M.P., 2000, ApJ, 532, 895
- Bower, G.A., Wilson, A.S., Heckman, T.M., & Richstone, D.O., 1996, AJ, 111, 1901
- Capriotti, E., Foltz, C., & Byard, P., 1980, ApJ, 241, 903
- Capriotti, E., Foltz, C., & Byard, P., 1980, ApJ, 245, 396
- Chen, K., & Halpern, J.P., 1989, ApJ, 344, 115
- Collin-Souffrin, S., & Lasota, J.P, 1988, PASP100, 1041
- Devereux, N., Ford, H., & Jacoby, G., 1997, ApJ, 481, 71
- Devereux, N., Ford, H., Tsvetanov, Z., & Jacoby, G., 2003, ApJ, 125, 1226
- Edelson, R.A., & Krolik, J.H., 1988, ApJ, 333, 646
- Eracleous, M., & Halpern J.P., 2001, ApJ, 554, 2406
- Eracleous, M., & Halpern J.P., 2003, ApJ, 599, 886
- Ferrarese, L., & Merritt, D., 2000, ApJ, 539, L9
- Filippenko, A.V., & Sargent, W.L.W., 1985, ApJS, 57, 503
- Filippenko, A.V., & Sargent, W.L.W., 1988, ApJ, 324, 134

- Freedman, W.L., et al. 2001, ApJ, 553, 47
- Greene, J.E., & Ho, L.C., 2005, ApJ, 630, 122
- Hazard, C.; Morton, D. C.; Terlevich, R.; McMahon, R., 1984, ApJ, 282, 33
- Ho, L.C., Filippenko, A.V., & Sargent, W.L.W., 1996, ApJ, 462, 183
- Kaspi, S., Maoz, D., Netzer, H., Peterson, B.M., Vestergaard, M., & Jannuzi, B.T., 2005, ApJ, 629, 61
- King, A., & Pounds, K., 1981, MNRAS, 347, K657
- Kwan, J., & Krolik, J.H., 1981, ApJ, 250, 478
- La Parola, V., Fabbiano, G., Elvis, M., Nicastro, F., Kim, D.W., & Peres, G., 2004, ApJ, 601, 831
- Maoz, D., Koratkar, A., Shields, J.C., Ho, L.C., Filippenko, A.V., & Sternberg, A., 1998, AJ, 116, 55
- Mathews, W.G., & Ferland, G.J., 1987, ApJ, 323, 456
- Murry, N., & Chiang, J., 1997, ApJ, 474, 91
- Peimbert, M., & Torres-Peimbert, S. 1981, ApJ, 245, 845
- Peterson, B., 1993, PASP, 105, 247
- Peterson, B., 2001, in Advanced Lectures on the Starburst-AGN Connection, ed. I. Aretxaga, D. Kunth, & R. Mujica (Singapore: World Sci.), 3
- Rees, M.J., 1977, QJRAS, 18, 429
- Robinson, A., & Perez, E., MNRAS, 244, 138
- Robinson, A., Perez, E., Binette, L., MNRAS, 246, 349
- Scoville, N., & Norman, C., 1988, ApJ, 332, 163
- Seyfert, C.K., 1943, ApJ 97, 28
- Shlosman, I., Vitello, P.A., & Shaviv, G., 1985, ApJ, 294, 96
- Zheng, W., Binette, L., & Sulentic, J.W., 1985, ApJ, 365, 115

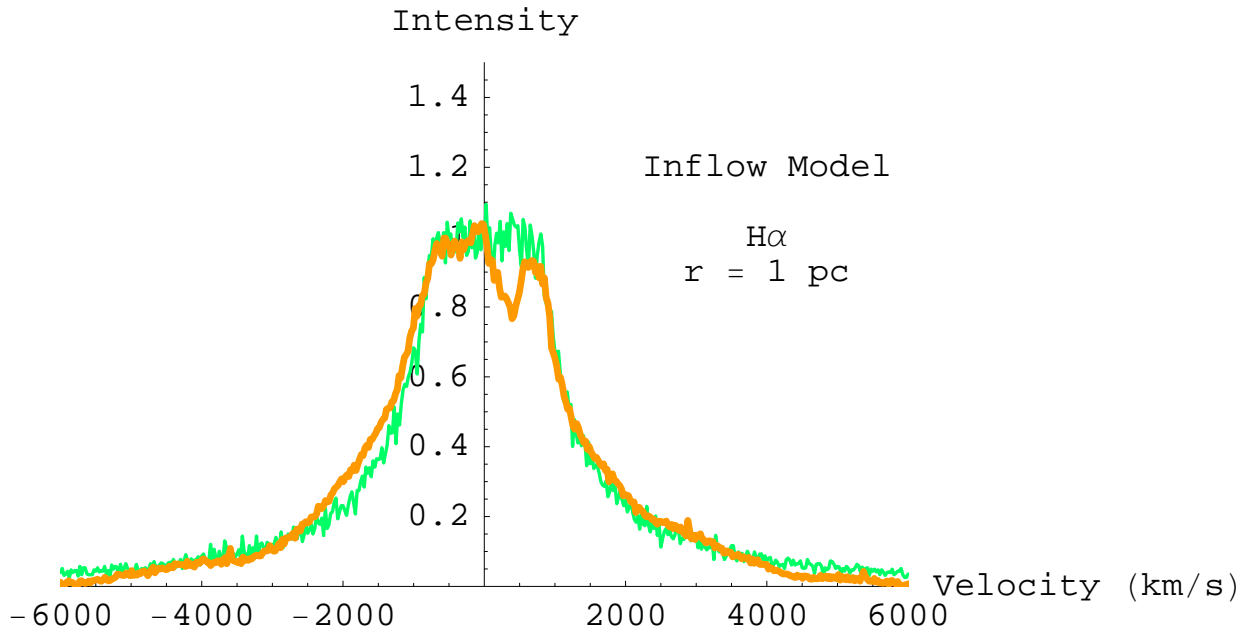


Fig. 1.— Broad H α emission line in M81. The observed profile (Devereux et al. 2003) is shown in orange and the inflow model is shown in green. The inflow was generated using 75,000 randomly distributed points in free-fall from an outer radius of 1 pc (see text for details). The intensity of both profiles has been normalized to the intensity at zero velocity.

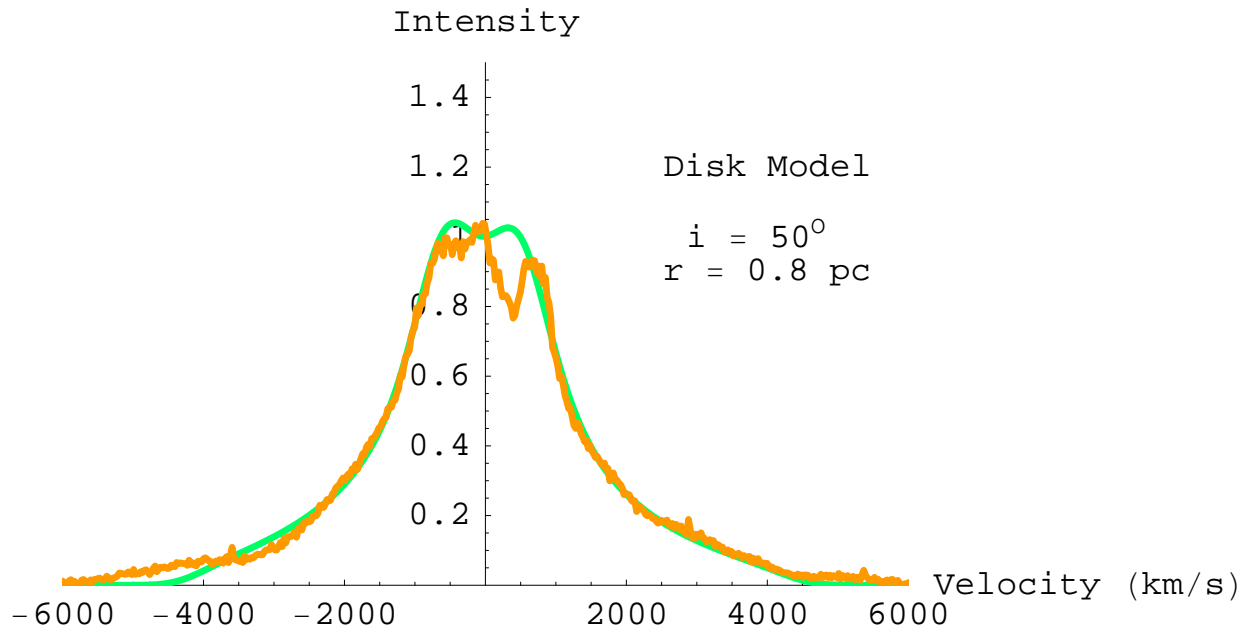


Fig. 2.— Observed Broad H α emission line in M81, shown in orange, with the disk model shown in green. The disk is 0.8 pc in radius and is inclined by 50 degrees to the line of sight (see text for details). The intensity of both profiles has been normalized to the intensity at zero velocity.

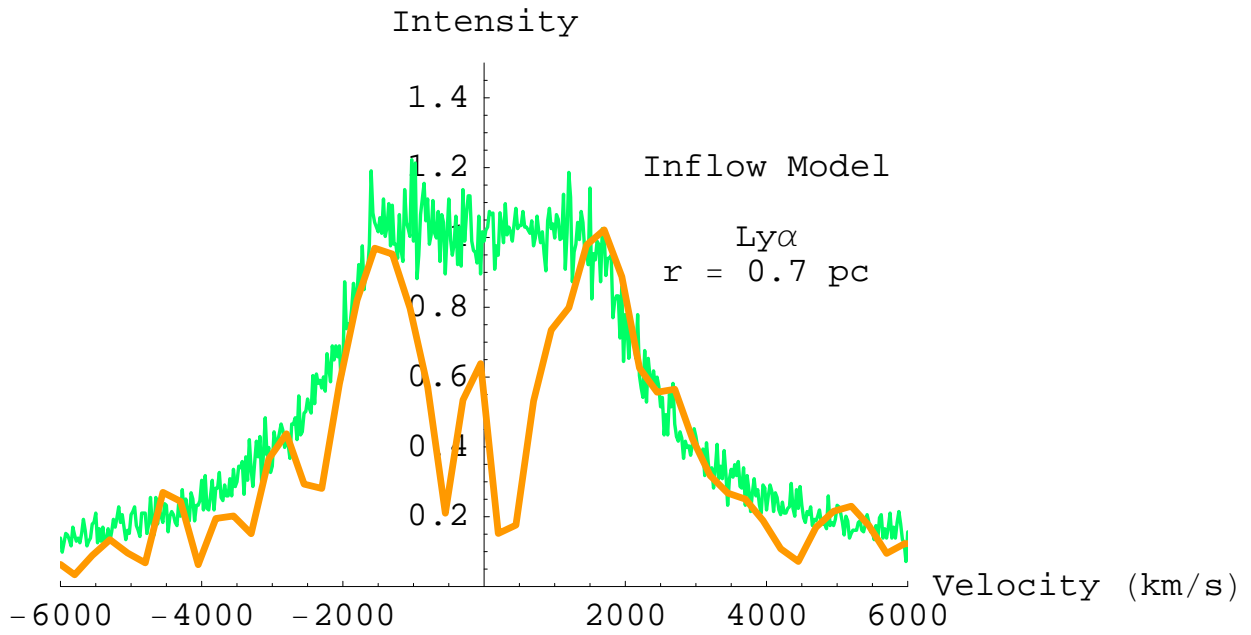


Fig. 3.— Broad $\text{Ly}\alpha$ emission line in M81. The observed profile (Ho, Filippenko & Sargent 1996) is shown in orange. The model profile, shown in green, represents an inflow (see text for details). The intensity of the model profile has been normalized to the intensity at zero velocity.

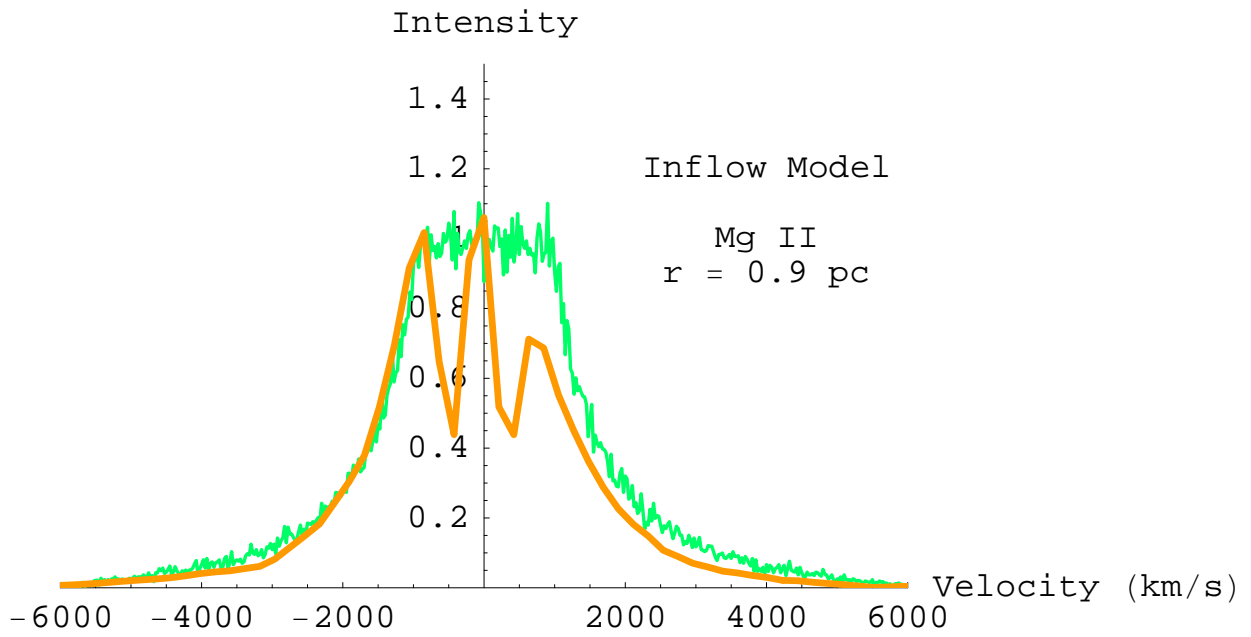


Fig. 4.— Broad Mg II emission line in M81. The observed profile (Ho, Filippenko & Sargent 1996) is shown in orange. The model profile, shown in green, represents an inflow (see text for details). The intensity of both profiles has been normalized to the intensity at zero velocity.